OncoTargets and Therapy

Dovepress
open access to scientific and medical research

Open Access Full Text Article

ORIGINAL RESEARCH

RETRACTED ARTICLE: Effects of miR-330-3p on Invasion, Migration and EMT of Gastric Cancer Cells by Targeting PRRX1-Mediated Wnt/β-Catenin Signaling Pathway

This article was published in the following Dove Press journal:
OncoTargets and Therapy

Bingqiang Ma*
Jianxun Ma*
Yili Yang
Xueyuan He
Xinmin Pan
Zhan Wang
Yaowen Qian

Department of General Surgery, Cancer Center, Key Laboratory for Diagnosis and Treatment of Gastrointestinal Cancer, Gansu Provincial Hospital, Lanzhou, Gansu Province, People's Republic of China

*These authors contributed equally to this work

Background: miRNA, as a biological marker, had mo and more a tion in cent years due to the important role it plays in cancer. Currently, th are exte ive stu on miRNAs, among which miR-330-3p is reported to be implicated in e pa ophysiological processes of various cancers. However, little progress has been m e in the m anism o iR-330-3p in gastric cancer.
Objective: To explore the expression relevant mec n of miR-330-3p and PRRX1 in gastric cancer (GC).
Methods: Forty-five GC patie study group), om whom paired GC and paracancerous tissues were collected, and another 45 healthy subjects (control group) who underwent physical examination dur g the same riod were enrolled. In addition, GC cells and human gastric mucosa c were pu hased, and miR-330-3p-mimics, miR-330-3p-inhibitor, miR-N si-PRRX1, d sh RRX1 were transfected into MKN45, SGC7901 cell. QRT-PCR w s em ed to assess the miR-330-3p and PRRX1 expressions in the samples, and the c ll e pressi s of PRRX1, GSK-3β, p-GSK-3β, β-catenin, p-β-catenin, cyclin cadher E-cadherin and vimentin were evaluated by Western blot (WB). MTT, Tr swell an wound- aling experiments were adopted to detect cell proliferation, invasion a migra
Resu MiR-330-3p was under-expressed, while PRRX1 was highly expressed in the serum of patients, h of which had an area under the curve (AUC) of more than 0.9. MiR-330-3p and PRRX1 were associated with tumor diameter, TNM staging, lymph node metastasis and differ- ation of GC patients. Overexpression of miR-330-3p and inhibition of PRRX1 expression coul suppress epithelial–mesenchymal transition (EMT), proliferation, invasion and apoptosis of cells. What is more, WB assay showed that overexpressed miR-330-3p and inhibited PRRX1 could inhibit the expression levels of p-GSK-3β, β-catenin, cyclin D1, N-cadherin and vimentin proteins, while elevating GSK-3β, p-β-catenin and E-cadherin protein expressions. Dual-luciferase reporter assay confirmed that there was a targeting relation between miR-330-3p and PRRX1. Furthermore, rescue experiments revealed that the cell proliferation, invasion, migration did not differ significantly between co-transfected miR-330-3p-mimics+sh-PRRX1, miR-330-3p-inhibitor+si-PRRX1 groups of MKN45 and SGC7901 and the miR-NC group (without transfected sequences).
Conclusion: Overexpressed miR-330-3p can promote cell EMT, proliferation, invasion and apoptosis through inhibiting PRRX1-mediated Wnt/β-catenin signaling pathway, which is expected to be a potential therapeutic target for GC.

Keywords: miR-330-3p, PRRX1, Wnt/β-catenin signaling pathway, biological function, GC

Introduction

Characterized by early metastasis and poor prognosis in the late stage, gastric cancer, as a common malign tumor of the digestive system, presents an increased

Correspondence: Yaowen Qian
General Surgery, Cancer Center, Key Laboratory for Diagnosis and Treatment of Gastrointestinal Cancer, Gansu Provincial Hospital, 204 Donggangxi Road, Chengguan District, Lanzhou, Gansu Province 730000, People's Republic of China
Tel +86 15293110056
Email qyw2218@163.com

morbidity and mortality along with the changes of the social environment and dietary habits.[1–3] Currently, surgery and chemotherapy remain the primary treatment approaches for patients with GC, however, with poor and unsatisfactory outcomes. For your consideration, the five-year survival rate accounts less than 30%.[4] In view of the unfavorable situation, finding a biomarker with high sensitivity to the diagnosing and treating of gastric cancer has important clinical significance for patients with gastric cancer.

In recent years, the molecular mechanism of miRNA in tumor has been a research hotspot in cancer-related fields. miRNA, as a small non-coding RNA, can adjust and control target genes' expression by binding to the 3′UTR of its target genes.[5,6] Among which, miR-330-3p refers to a miRNA with abnormal expression in varying tumor cells. For example, studies[7] showed that it could accelerate the cell metastasis of breast cancer by targeting CCBE1. Others[8] supported that miR-330-3p was able to inhibit the migration of liver cancer cells by targeting MAP2K1. Although such research demonstrated that miR-330-3p was extensively involved in various tumors, the specific mechanism of its action in GC had not been elaborated. PRRX1 is a homeobox protein and an inducer of epithelial–mesenchymal transition (EMT).[9] Previous findings displayed that PRRX1 could promote the EMT process of GC cells by mediating the transmission of Wnt/β-catenin signal pathway.[10] As regard to Wnt/β-catenin, also belongs to a classical signaling pathway in the pathological process of tumor, which is over-expressed in tumor cells and has some certain effects on the proliferation and apoptosis.[11]

PRRX1 was supposed to be a potential target site for miR-330-3p through online biological prediction software (http://www.targetscan.org/vert_72/). Based on previous research, we speculated that miR-330-3p could affect the biological function of cells by targeting Wnt/β-catenin signaling pathway mediated by PRRX1, and thus the following research was conducted.

Data and Methods

Clinical Data

Totally 45 patients with GC treated in our hospital from March 2015 to June 2018 were selected as the study group, including 25 male and 20 female, averagely aged (57.4±3.1) years. Forty-five paired cases of gastric cancer tissues and paracancerous tissues were obtained as research specimens during the resection of gastric cancer with the consent of the patients. Another 45 healthy subjects who had a physical examination in our hospital during the same period were assigned into the control group, including 24 males and 21 females, averagely aged (57.5±3.3) years. Though comparable, it was obvious that no significant difference existed in terms of gender and age between the two groups (P>0.05). The inclusion criteria were as follows: All patients enrolled in the study group were diagnosed as GC by pathological diagnosis with an expected survival of more than 3 months. The exclusion criteria were as follows: Patients with severe liver and kidney dysfunction. Patients with other malignant tumors. Patients who had received any treatment before the experiment. Patients with infection or immunity and patients with systemic diseases. All patients and their families agreed to participate in the experiment and written informed consents were obtained. This experiment has got the approval of the Medical Ethics Committee of Gansu Provincial Hospital and Committee on the Ethics of Animal Experiments of Gansu Provincial Hospital, and this study is in line with the Declaration of Helsinki.

Reagents and Materials

MKN-28, MKN-45, MGC-803, SGC-7901 of Human GC cells and GES of human normal gastric mucosal cell lines were acquired from Bena Culture Collection, Beijing, China, Subordinate agent of ATCC, with the item number of 41,748, 337,682, 100,665, 100,114, 337,970, respectively. TransScript Green miRNA Two-Step qRT-PCR SuperMix and TransScript II Green Two-Step qRT-PCR SuperMix kits were purchased from TransGen Biotech Co., Ltd., Beijing, China, with the corresponding item number of AQ202-0 1, AQ301-01. The MTT, dual-luciferase reporter gene assay kit and RIPA was obtained from Biolab Technology Co., Ltd., Beijing, China, with the item number of SY0502, KFS303, JN0190, respectively. The Transwellkit, PBS and FBS were all acquired from Gibco Co., USA, with the item number of 1,142,802, 10,010,049, 10,437,028, respectively. The BCA protein kit was acquired from Thermo Scientific Company, with the item number of A53225, and Trizol kit from Invitrogen with the item number of 10,296,010. The PRRX1, GSK-3β, p-GSK-3β, β-catenin, p-β-catenin, cyclin D1, N-cadherin, E-cadherin, vimentin and β-Actin antibodies were all obtained from Cell Signaling Technology Company. The goat anti-rabbit IgG antibody was purchased from Boster Biological Technology Co., Ltd., Wuhan, China, ECL developer from Thermo Company, and PCR7500 from ABI Company, USA.

Sangon Biotech (Shanghai) Co., Ltd. was responsible for the design and synthesis of all primers.

Cell Culture, Passage and Transfection

GC cell lines were cultured in a medium containing 10% PBS DMEM at 37°C with 5% CO_2. When the cell adherent growth and fusion reached 85%, 25% trypsin was added for digestion. After that, GC cell lines were placed in the medium for further culture, passage, and finally cell transfection. MiR-330-3p-inhibitor (suppression sequence), miR-330-3p-mimics (overexpression sequence), miR-negative control (miR-NC), PRRX1 RNA (si-PRRX1), PRRX1 RNA (sh-PRRX1), negative control RNA (NC) were transfected by Lipofectamine™ 2000 kit, and the procedures were carried out strictly according to the kit instructions.

Detection Method

QRT-PCT Detection

Serum and cells were collected and TRIzol kit was used to abstract the total RNA, whose purity and concentration was detected by ultraviolet spectrophotometer. Then, 5μg of the total RNA was taken for cDNA reverse transcription according to the kit instructions, followed by the amplification of the synthesized cDNA (1μg). The miR-330-3p amplification system: cDNA: 1μL, upstream and downstream primers: 0.4 μL, respectively, 2×Taq® Green qPCR SuperMix:10 μL, Passive Reference Dye (50X): 0.4 μL, and ddH2O was added to 20μL. The amplification conditions were as follows: The PCR reaction conditions were pre-denaturation at 94°C for 30 s, then denaturate at 94°C for 5 s and then annealing at 60°C for 30 s, and the operation was repeated for a total of 40 cycles. The PRRX1 amplification system: cDNA: 1 μL, upstream and downstream primers: 0.4 μL, respectively, 2X TransScript® Green qPCR SuperMix: 10 μL, Passive Reference Dye (50X): 0.4 μL, and added Nuclease-free Water to complete 20μL. The amplification conditions were stated as below: Pre-denaturation: 95°C/30 s, denaturation: 95°C/5 s, annealing: 60°C/30 s, totaling 40. Three repeat holes were set for each sample, and the experiment was carried out for a total of 3 times. U6 was represented as the internal reference for miR-330-3p, β-Actin as the internal reference for PRRX1, and $2^{-\Delta\Delta ct}$ was employed to analyze the data.

Immunohistochemical Experiment

First, the tissue was embedded in paraffin and sectioned, and then stained according to the experimental procedure. Next, the tissue sections were incubated at room temperature and 3% $H2O_2$ for 20 min to remove endogenous peroxidase activity, and then washed with PBS. Then, the sections were incubated with PRRX1 primary antibody at 4°C overnight. After PBS washing, the sections and horseradish peroxidase-labeled goat anti-rabbit IgG were placed at room temperature for 30 min. Then, the sections were re-rinsed with PBS, and incubated with the solution of streptomycin antibiotic protein peroxidase at 37°C for 10 min. Under the microscope, the sections developed with the freshly prepared diaminobenzidine were observed for 20 s. After re-dyeing with hematoxylin, the sections were rinsed with water for 15 min, dehydrated with ethanol, and then cleared of xylene and sealed with neutral gum. Followed by the observation of staining under the microscope. After re-dyeing with hematoxylin, the sections were rinsed with water for 15 min, dehydrated with ethanol, then cleared of xylene and sealed with neutral gum. Finally, the staining was observed under the microscope.

Western Blot Detection

RIPA lysate was added to the cells of each group after culture, and the total protein in the cells was extracted. Then, the protein concentration was detected by BCA assay. The protein concentration was adjusted to 4ug/μL, electrophoretically separated by 12% SDS-PAGE before transferring to PVDF membrane, and then sealed by 5% skim milk powder for 2 h. Next, PRRX1 (1:500), GSK-3β (1:500), p-GSK-3β (1:500), β-catenin (1:500), p-β-catenin (1:500), cyclin D1 (1:500), N-cadherin (1:500), E-cadherin (1:500), vimentin (1:500) and β-Actin I antibody (1:1000) were added and sealed overnight at 4°C. After that, the membrane was washed to remove the primary antibody, followed by the adding of horseradish peroxidase-labeled goat anti-rabbit secondary antibody (1:500), incubated at 37°C for 1 h, and rinsed with PBS for 3 times, 5 min each. Developed in a dark room, dried the extra liquid on the membrane with filter paper, and developed with ECL luminescence. Finally, the protein bands were scanned and analyzed in Quantity One software for grayscale value, where the relative protein expression = grayscale value of the target protein bands/grayscale value of the β-Actin protein bands.

MTT Assay for Cell Viability

After 24-h transfection, cells were collected and adjusted to $5*10^3$cells, inoculated on 96-well plates, and cultured for 24 h, 48 h and 72 h. At each time point, 20μL MTT solution (5μL/mL) was added to each well for 4 h of continuous

culture at 37°C, and the 200μL dimethyl sulfoxide was added. At last, OD value of each group was then assessed by a spectrophotometer at 570 mm wavelength.

Transwell Detection

Cells were collected 24 h after transfection, and its density was adjusted to $3*10^4$ cells/well. Then, the cells were inoculated in 24-well plates, digested with trypsin, and transferred to the upper chamber, where 200μL RPMI1640 culture solution was added, and 500μL RPMI1640 (with 10% FBS) was added into the lower chamber, then cultured at 37°C for 48 h. The stroma and cells failed to cross the membrane surface were wiped and rinsed with PBS for 3 times, followed by a 10-min fixing with paraformaldehyde, and then washed with double-steamed water for 3 times. After drying, they were stained with Crystal Violet Stain Solution with a concentration of 0.5%, and the cell invasion was observed using a microscope.

Wound-Healing Assay for the Observation of Cells' in vitro Migration Ability

The cells were diluted to 3 x 10^5 cells/mL and inoculated in 6-well plates. When the cells grew to 85%, the cells were divided into a cell-free area by p200 Pipet tips. Then, the wounded cells were rinsed with PBS and added to the new medium for culture, whose migration ability was measured by the healing of three different wound sites at 0 h (W0) and 24 h (W24) using a microscope.

Dual-Luciferase Reporter Assay

The 3′-UTR of PRRX1 containing the miR-330-3p putative binding site was amplified and subcloned into the pGL3 luciferase promoter vector (Promega Corporation, Fitchburg, WI, USA). Then, the vector combined with miR-330-3p mimics was co-transfected into 293T cells for 48 h. Then, the cells were harvested and tested for relative luciferase activity using the dual-luciferase reporting kit (Promega Corporation) according to the manufacturer's instructions. Subsequently, miR-330-3p-inhibitor, miR-330-3p-mimics, and control sequences were co-transfected into GC cells by Lipofectamine 3000 (Invitrogen, Thermo Fisher Scientific, USA). The effect of miR-330-3p on PRRX1 protein expression was detected by, Western Blot. All experiments were performed 3 times.

MS2-RNA Binding Protein Immunoprecipitation (RIP)

MS2-PRRX1-WT vector (containing miR-330-3p binding site) and MS2-PRRX1-MUT vector (without miR-330-3p binding site) with MS2 hairpin structure were constructed. The vectors were then transfected into gastric cancer cells. Forty-eight hours later, immunoprecipitation was performed using Magna RIPTM RNA-binding protein immunoprecipitation kit (Millipore). QPCR was adopted to quantify the expression of miR-330-3p.

Xenograft Model of Tumor in Nude Mice

Female BALB/c nude mice aged 4-weeks old were raised in a sterile environment, and then $3x10^6$ MDN-45 cells of the stable miR-330-3p-mimics and its control plasmid were subcutaneously injected into the left abdomen of the nude mice. The nude mice were grouped with 5 each, whose tumor growth was detected every 7 days. After 28 days of continuous injection, the mice were executed by cervical dislocation and the size and mass of the tumor in the body were precisely measured. Animal experiments are performed in accordance with the US Guide to Management and Use of Laboratory Animals. This experiment has been declared through animal experiment ethics。

Statistical Methods

The collected data were statistically analyzed using SPSS 20.0 software and plotted by GraphPad 7 in the current study. An independent sample *t*-test was adopted for inter-group comparison. One-way ANOVA was employed for multi-group comparisons and expressed as F. LSD-*t* test was used for post-hoc pairwise comparison, and repeated measurement ANOVA was used for multiple time points, represented by F. Bonferroni was used for post-test verification and ROC was adopted to map the diagnostic significance of miR-330-3p and PRRX1 in GC. Pearson test was conducted to analyze the relation between the expression of miR-330-3p and PRRX1 in the serum of patients. K-M survival curve was used to plot the 3-year survival of the patients and Log-rank test for analysis. A statistically significant difference was assumed at $P<0.05$.

Results

Expression and clinical value of miR-330-3p and PRRX1 in the serum of GC patients

The serum miR-330-3p and PRRX1 expressions of the participants were detected, it was found that the study group had a significantly decreased miR-330-3p expression and a markedly increased PRRX1 expression than those of the control group, which was statistically different ($P<0.05$). In addition, the expression detection of miR-330-3p and PRRX1 in patients' tissues showed that, compared with paracancerous tissues, the miR-330-3p

expression was noticeably lower while the PRRX1 expression was remarkably higher in the GC tissues. Immunohistochemical detection also revealed that the positive rate of PRRX1 in GC tissues was significantly higher than that in paracancerous tissues. Pearson's analysis demonstrated that the expression of miR-330-3p and PRRX1 in the serum of GC patients was negatively correlated (P<0.05). According to ROC curve, the AUC of miR-330-3p and PRRX1 was 0.944 and 0.920, respectively. Further analysis of the relationship between these two indicators and the pathological data of patients demonstrated that miR-330-3p and PRRX1 were bound up with tumor diameter, differentiation degree, TNM staging, as well as lymph node metastasis (P<0.05). (Table 1, Figure 1)

Effects of miR-330-3p on Proliferation, Invasion, Migration and EMT of GC Cells

The detection of miR-330-3p expression in GC cells revealed that, in contrast with normal gastric mucosal cells, MKN-28, MKN-45, MGC-803 and SGC-7901 of human GC cell lines presented a markedly reduced miR-330-3p expression (P<0.05). After transfecting miR-330-3p-mimics, miR-330-3p-inhibitor and miR-NC into MKN-45 and MGC-803 cells, the miR-330-3p expression of miR-330-3p-mimics transfected cells was markedly elevated, while that of miR-330-3p-inhibitor-transfected cells substantially decreased in comparison with the cells transfected with miR-CN. In addition, the miR-330-3p-mimics transfected cells displayed significantly reduced, and the miR-330-3p-inhibitor-transfected cells showed the markedly elevated ability of cell proliferation, invasion and migration than miR-CN transfected cells. In the biological function detection of the two groups. What is more, the expressions of GSK-3β, β-catenin, cyclin D1, N-cadherin, vimentin were significantly reduced, and GSK-3β, p-β-catenin and E-cadherin expressions were markedly enhanced after miR-330-3p-mimics transfection compared to miR-NC transfected cells, while the case was reversed after transfecting with miR-330-3p inhibitor (Figure 2).

Table 1 Correlation Between miR-330-3p, PRRX1 and Pathological Data of GC Patients

Factors		Relative Expression of miR-330-3p	t value	P value	Relative Expression of PRRX1	t value	P value
Gender	Male (n=25)	0.61±0.13	1.398	0.169	1.57±0.24	0.278	0.783
	Female (n=20)	0.63±0.13			1.59±0.24		
Age (years)	<57 (n=23)	0.66±0.11	1.395	0.170	1.60±0.23	0.571	0.571
	≥57 (n=22)	0.61±0.13			1.56±0.24		
TNM staging	I, II (n=26)	0.72±0.07	8.913	<0.001	1.42±0.12	8.277	<0.001
	III, IV (n=19)	0.52±0.08			1.79±0.18		
Tumor diameter	≥5cm (n=21)	0.55±0.09	5.950	<0.001	1.75±0.19	6.485	<0.001
	<5cm (n=24)	0.71±0.09			1.43±0.14		
Lymph node metastasis	Transferred (n=18)	0.53±0.08	6.482	<0.001	1.73±0.20	4.108	<0.001
	Non-transferred (n=27)	0.70±0.09			1.48±0.20		
Differentiation degree	Low differentiation (n=25)	0.56±0.10	5.333	<0.001	1.71±0.20	5.567	<0.001
	Medium-high differentiation (n=20)	0.72±0.10			1.41±0.15		

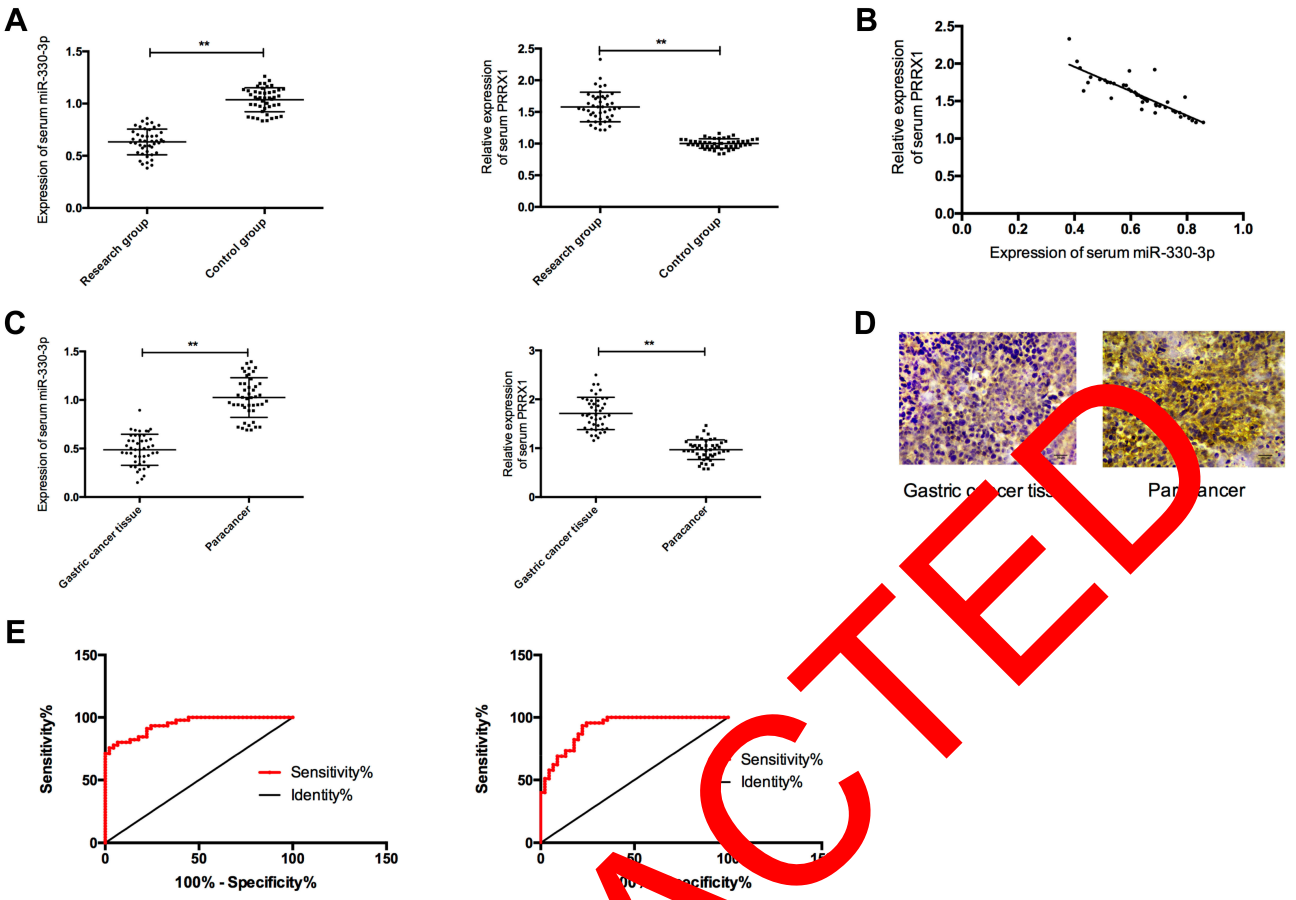

Figure 1 Expression and clinical value of serum RNA-330-3p and PRRX1 in GC patients. (**A**) The expression of miR-330-3p was low while PRRX1 was high in the serum of GC patients. (**B**) The serum expression of miR-330-3p and PRRX1 showed a negative correlation in GC patients. (**C**) MiR-330-3p was lowly expressed while PRRX1 was highly expressed in GC tissues. (**D**) The positive rate of immunohistochemical detection of PRRX1 in GC tissues was significantly higher than in paracancerous tissues. (**E**) The AUC of miR-330-3p curve was 0.944, and that of the PRRX1 was 0.9[illegible].**Indicate P <0.05.

Effects of PRRX1 on Proliferation, Invasion, Migration and EMT of GC Cells

The expression of PRRX1 in human GC cell lines represented by MKN-28, MKN-45, MGC-803 and SGC-7901 was substantially elevated than that of GES in normal gastric mucosa cell lines ($P<0.05$). While after transfection of MKN-45 and SGC-803 cells with si-PRRX1, sh-PRRX1 and miR-NC, the expression of PRRX1 in the si-PRRX1 transfected cells with MKN-45 and MGC-803 was significantly reduced, and that of the sh-PRRX1 transfected cells with EC109 and EC9706 was significantly increased than NC transfected cells ($P<0.05$). Additionally, the biological functions detection revealed that compared to the NC transfected cells, the proliferation, invasion and migration of si-PRRX1 transfected cells were substantially abated, while those of the sh-PRRX1 transfected cells significantly increased ($P<0.05$). Moreover, the expressions of p-GSK-3β, β-catenin, cyclinD1, N-cadherin vimentin were substantially abated after transfection of si-PRRX1, and the GSK-3β, p-β-catenin and E-cadherin expressions were significantly increased in si-PRRX1 transfected cells in contrast with NC transfected cells, while the case was reversed in cells transfected with sh-PRRX1 ($P<0.05$). (Figure 3)

Target Gene Identification of miR-330-3p

For further verifying the relationship between miR-330-3p and PRRX1, the target binding site between PRRX1 and miR-330-3p was detected by predicting the downstream target gene of miR-330-3p through Targetscan7.2. What is more, dual-luciferase reporter assay displayed that overexpressed miR-330-3p remarkably downregulated the luciferase activity of pmirGLO-PRRX1-3 'UT Wt ($P<0.05$), but had no effect on that of pmirglo-PRRL1-3′ UTR Mut ($P>0.05$). Furthermore, WB detection revealed that PRRX1 expression was markedly reduced in MKN-45 and MGC-803 cells after transfection with miR-330-3p-mimics, and

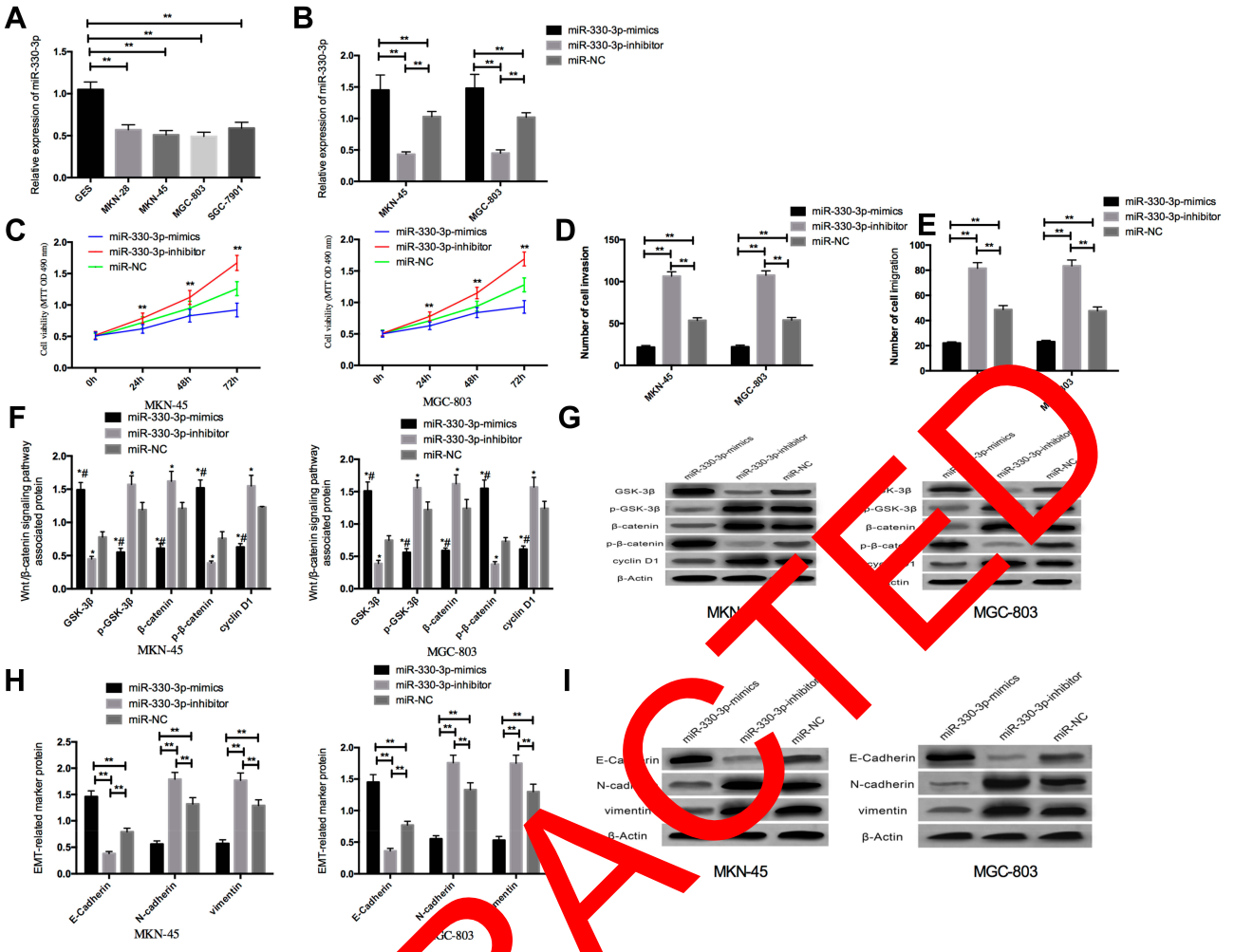

Figure 2 Effects of miR-330-3p on proliferation, invasion, migration of GC cells. (**A**) MiR-330-3p presented low expression in GC cells. (**B**) The miR-330-3p expression was substantially elevated in miR-330-3p-mimics transfected cells, and markedly abated in miR-330-3p-inhibitor-transfected cells. (**C**) The proliferation ability of miR-330-3p-mimics transfected cells was markedly reduced, while that of miR-330-3p-inhibitor-transfected cells was dramatically increased. (**D**) The invasion ability of miR-330-3p-mimics transfected cells was markedly reduced, while that of miR-330-3p-inhibitor-transfected cells was substantially increased. (**E**) The migration ability of miR-330-3p-mimics transfected cells was substantially reduced, while that of miR-330-3p-inhibitor-transfected cells was markedly boosted. (**F**) The p-GSK-3β, β-catenin and cyclinD1 expressions in miR-330-mimics cells were markedly abated, with significantly increased expressions of GSK-3β, p-β-catenin and cyclinD1, while the expressions were reversed in the miR-330-3p-inhibitor-transfected cells. (**G**) Western Blot. (**H**) The N-cadherin and vimentin expressions were substantially decreased, and expression of E-cadherin was significantly increased in miR-330-3p-mimics transfected cells, while expression of N-cadherin and vimentin was significantly increased, and the E-cadherin expression was markedly decreased in miR-330-3p-inhibitor-transfected cells. (**I**) Western Blot. **Indicated P<0.05, *Indicated P<0.05 in contrast with the miR-NC group. #Indicated P<0.05 in contrast with the miR-330-3p-inhibitor group.

substantially elevated after transfecting miR-330-3p-inhibitor (P<0.05). (Figure 4)

Rescue Experiments

Further co-transfection of miR-330-3p-mimics+sh-PRRX1 or miR-330-3p-inhibitor+si-PRRX1 into MKN-45, MGC-803 cells revealed no significant difference in proliferation, invasion and migration between the two and when in contrast with the miR-NC group. However, comparing to miR-330-3p-mimics, miR-330-3p-mimics +sh-PRRX1 and miR-330-3p-inhibitor+si-PRRX1 showed significantly increased proliferation, invasion and migration ability (P<0.05), while presented significantly decreased ones compared with miR-330-3p-mimics (P<0.05). EMT-related protein detection revealed that there was no significant difference in the E-cadherin, N-cadherin and vimentin expressions in miR-330-3p-mimics+sh-PRRX1 and miR-330-3p-inhibitor+si-PRRX1 than those of the miR-NC group (P>0.05). When compared with miR-330-3p-mimics, E-cadherin expression of miR-330-3p-mimics + sh-PRRX1 and miR-330-3p-inhibitor+si-PRRX1 was significantly reduced, while N-cadherin and vimentin expression were markedly elevated. While compared with the miR-330-3p-inhibitor,

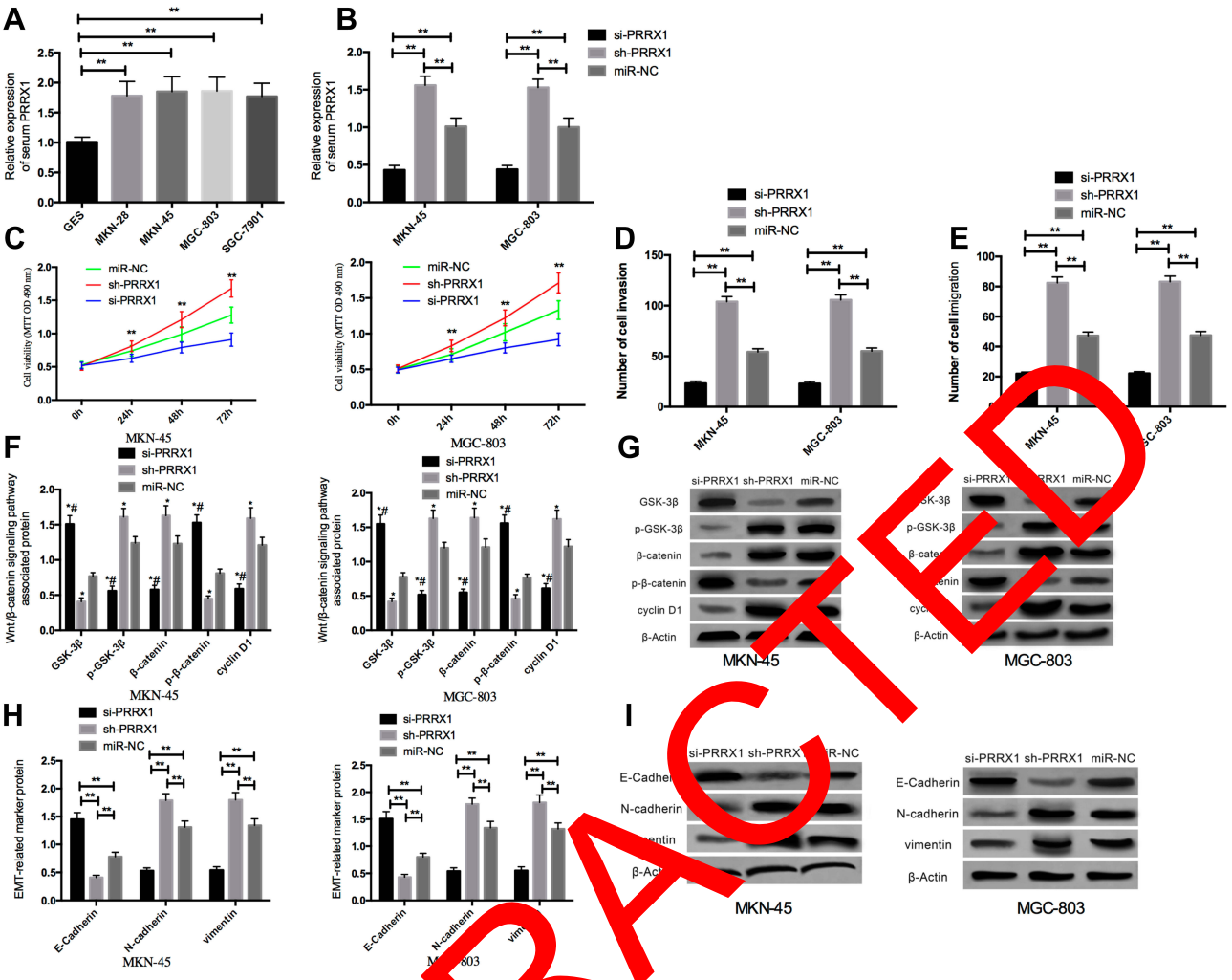

Figure 3 Effects of PRRX1 on proliferation, invasion, migration and EMT of GC cells. (**A**) PRRX1 was highly expressed in GC cells. (**B**) PRRX1 expression was substantially abated in sh-PRRX1 transfected cells and markedly decreased in si-PRRX1 transfected cells. (**C**) The proliferation ability of si-PRRX1 transfected cells was dramatically reduced, while that of sh-PRRX1 transfected cells was substantially increased. (**D**) The invasion ability of si-PRRX1 transfected cells was markedly reduced, while that of sh-PRRX1 transfected cells was significantly increased. (**E**) The migration ability of si-PRRX1 transfected cells was substantially reduced, while that of sh-PRRX1 transfected cells was markedly increased. (**F**) The p-GSK-3β, β-catenin, cyclin D1 expressions were significantly reduced, GSK-3β, p-β-catenin markedly boosted in cells transfected with si-PRRX1, while reversed in cells transfected with sh-PRRX1. (**G**) Western Blot. (**H**) The N-cadherin and vimentin expressions were substantially abated, and E-cadherin markedly boosted in the si-PRRX1 transfected cells. While the N-cadherin and vimentin expressions were markedly boosted, and E-cadherin was dramatically abated in sh-PRRX1 transfected cells. (**I**) Western Blot. **Indicated P<0.05. *Indicated P<0.05 in contrast with the miR-NC group. #Indicates P<0.05 in contrast with the sh-PRRX1 group.

miR-330-3p mimics + sh-PRRX1 and miR-330-3p-inhibitor + si-PRRX1 markedly boosted E-cadherin expression, and significantly reduced expressions of N-cadherin and vimentin (Figure 5).

Overexpressed miR-330-3p Inhibited Tumor Growth in Nude Mice

Tumor formation model was constructed by injecting MKN-45 cells transfected with miR-330-3p-mimics and miR-NC into the abdomen of nude mice. The results showed that there was a markedly lower tumor growth rate in the miR-330-3p-mimics group than that of the miR-NC group, so was the case with the tumor size and mass after the execution of nude mice (P<0.05), suggesting that overexpressed miR-330-3p can inhibit the tumors grow in vivo (Figure 6).

Discussion

Gastric cancer (GC) is a common malignancy of digestive system, whose poor prognosis largely results from its inconspicuous symptoms and metastasis in early stage.[12] In recent years, miRNAs have been proved to act as tumor suppressor genes or pro-oncogene, whose abnormal expression is closely germane to the genesis and progression of tumors, and are thus generally considered as the target

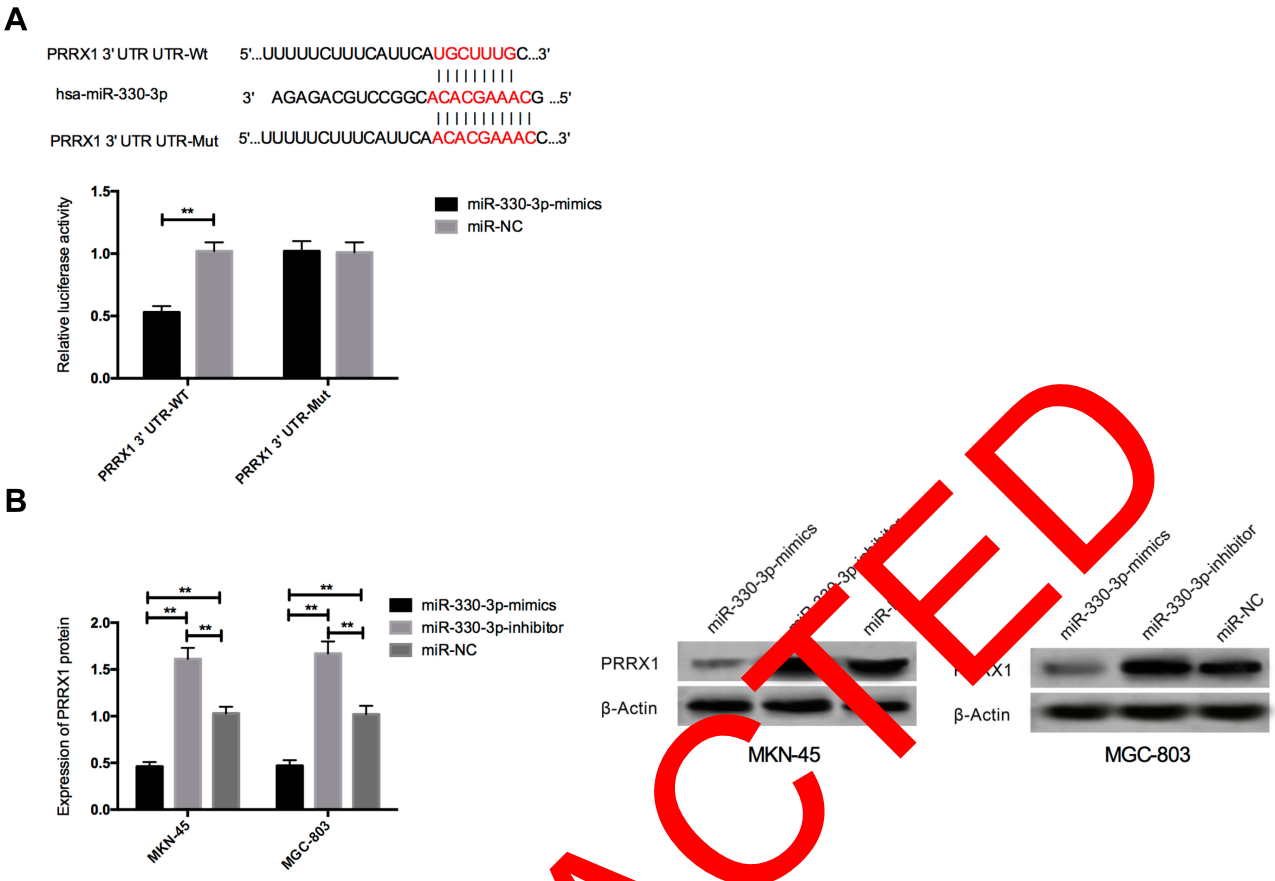

Figure 4 Dual-luciferase activity detection. (**A**) There was a binding point be[illegible]en mi[illegible]nd PRRX1: relative luciferase activity-dual luciferase reporter assay. (**B**) The expression of PRRX1 in MKN-45 and MGC-803 cells after transfection. **In[illegible]at[illegible] <0.05.

direction of cancer diagnosis or t[illegible]tment.[12] Previou[illegible] research demonstrated that miR-[illegible]0-3p[illegible] abnormally expressed in manifold kinds of [illegible]nors and ac[illegible]s oncogene promoter or suppressor. Fo[illegible] exam[illegible]le, studies [illegible] indicated that miR-330-3p was el[illegible]ated and co[illegible]d promote the proliferation of NSCL[illegible] cells by targeting EGR2. Others[15] revealed that thei[illegible]was a certain relevance between the abnormal expression [illegible] serum miR-330-3p of patients with leuk[illegible]mia as well as [illegible]nical outcomes of patients. Additi[illegible]ally, so[illegible] scholars[16] found that miR-330-3p was down-reg[illegible]d in GC tissues, and that miR-330-3p could inhibit the E[illegible]T of GC cells. The specific mechanism, however, has not elucidated yet.

Therefore, the clinical significance and potential molecular mechanism of miR-330-3p have been explored in the current study. Firstly, it was revealed that miR-330-3p was down-regulated in the serum and tissues of GC patients, which was consistent with previous studies. What is more, the decreased expression of miR-330-3p was found to be related to tumor diameter, differentiation degree, TNM staging and lymph node metastasis of GC patients when analyzing the clinical value of miR-330-3p. Moreover, the AUC curve of miR-330-3p was more than 0.9, indicating that miR-330-3p had a high diagnostic value for GC. Based on the above findings, it was suggested that miR-330-3p is strongly linked with the genesis and progression of GC, so cell experiments were further carried out.

To begin with, the expression of miR-330-3p in GC cell lines was determined to be markedly down-regulated by GES in contrast with normal gastric mucosa cells, which validated the results of the current study. Then, the up-regulation and down-regulation of miR-330-3p in MKN-45 and MGC-803 cells showed that the proliferation, invasion and migration ability of MKN-45 and MGC-803 cells transfected with miR-330-3p-mimics were remarkably suppressed, the N-cadherin and vimentin expression of EMT-related proteins were substantially abated, while the expression of E-cadherin was markedly boosted. However, the related expression of MKN-45 and MGC-803 cells after the transfection of miR-330-3p-inhibitor was contrary to that of miR-330-3p-mimics transfected ones, suggesting that miR-330-3p can be functioned

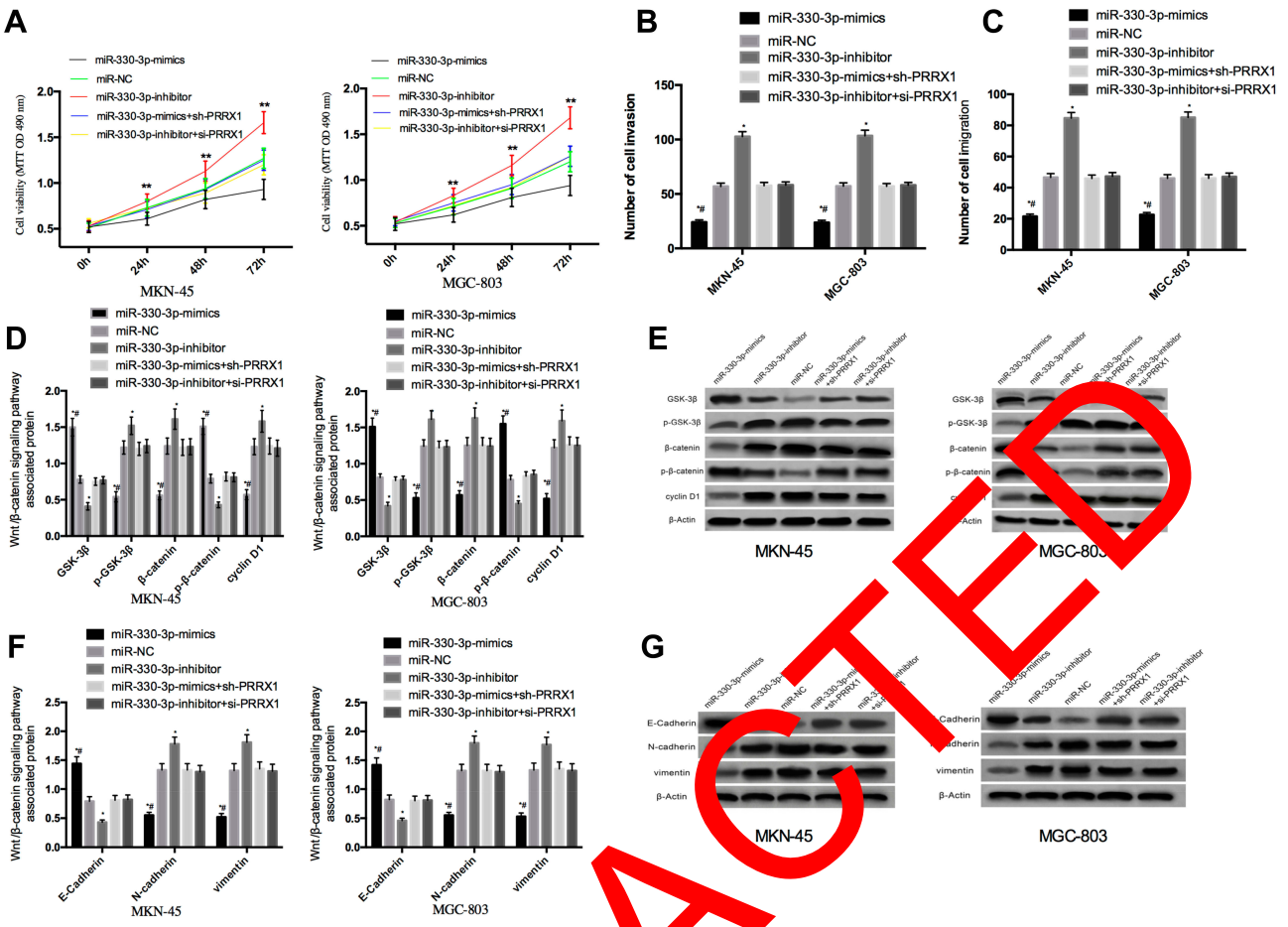

Figure 5 Rescue experiment. (**A**) Cell proliferation ability after transfection with miR-330-3p-mimics+sh-PRRX1 and miR-330-3p-inhibitor+si-PRRX1. (**B**) Cell invasion ability after transfection with miR-330-3p-mimics+sh-PRRX1 and miR-330-3p-inhibitor+si-PRRX1. (**C**) Cell migration ability after transfection with miR-330-3p-mimics+sh-PRRX1 and miR-330-3p-inhibitor+si-PRRX1. (**D**) P-GSK-3β, β-catenin, cyclin D1, GSK-3β and p-β-catenin expressions after transfection with miR-330-mimics+sh-PRRX1 and miR-330-3p-inhibitor+si-PRRX1. (**E**) Western Blot. (**F**) E-cadherin, N-cadherin and vimentin expressions after transfection with miR-330-3p-mimics+sh-PRRX1 and miR-330-3p-inhibitor+si-PRRX1. (**G**) Western Blot. *Indicated P<0.05 in contrast with miR-NC group, miR-330-3p-mimics+sh-PRRX1 group and miR-330-3p-inhibitor+si-PRRX1 group. #Represented P<0.05 in contrast with miR-330-3p-inhibitor.

as a potential target in GC treatment, and overexpressed miR-330-3p can inhibit cell proliferation, invasion, migration and EMT. In addition, the overexpressed miR-330-3p was found to be able to significantly promote the formation and growth of tumor through in vitro tumorigenesis in nude mice, which further suggested the significance of miR-330-3p in GC. However, how miR-330-3p affects the biological function and EMT of GC cells remains poorly understood.

The online target gene prediction website indicated that there were binding targets between PRRX1 and miR-330-3p. PRRX1 is a member of the homeostatic family, which exerts a marked effect in transcriptional activation and induction of downstream gene expression.[17] It has been reported that PRRX1, as one of the inducers of EMT, plays an essential part in the EMT process of different tumors as well as the invasion and metastasis of tumor cells.[18] In the current study, PRRX1 was highly expressed in the serum and tissues of patients with GC. Meanwhile, ROC curve analysis revealed that PRRX1 had a high diagnostic value for GC with the AUC of more than 0.9, and there was a strong connection between PRRX1 and tumor diameter, differentiation degree, TNM staging and lymph node metastasis, suggesting that PRRX1 may also be a potential diagnostic target for GC. Subsequently, the regulation of PRRX1 expression in MKN-45 and MGC-803 cells demonstrated that silencing PRRX1 could inhibit the EMT, proliferation, invasion and migration of GC cells, but the opposite results were observed after the overexpression of PRRX1. EMT has always been a hotspot in the study of tumor discovery mechanism, and the occurrence of EMT can weaken the connection between cells and promote their invasion and migration.[19] Therefore, it is speculated that silencing PRRX1 may inhibit the

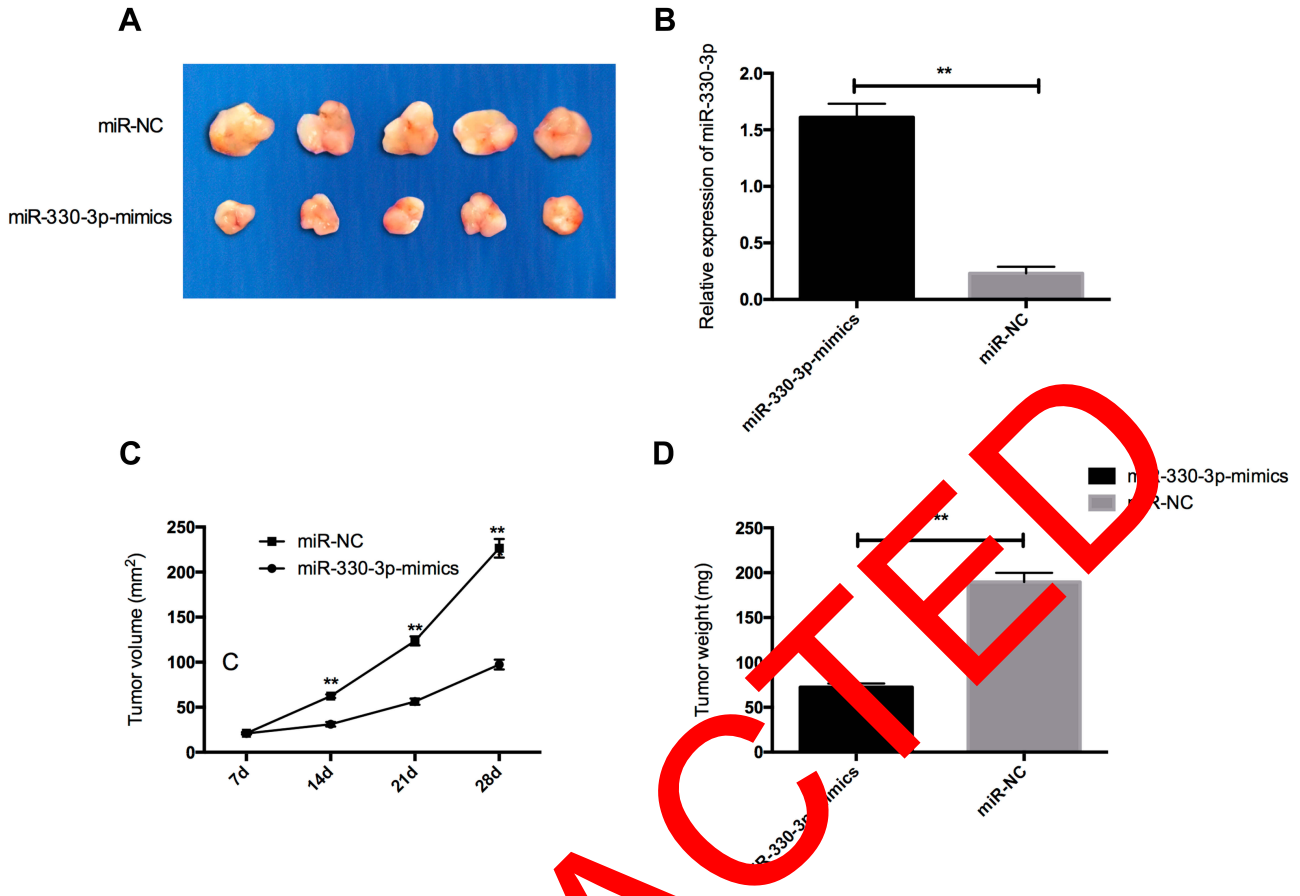

Figure 6 Effects of overexpressed miR-330-3p on tumor growth in nude mice. (**A**) Nude mice had smaller tumors in the miR-330-3p-mimics group than those in the miR-NC group. (**B**) MiR-330-mimics group presented a higher expression of miR-330-3p in tumor tissues than that of the control group. (**C**) The tumor growth rate in the miR-330-3p-mimics group was markedly slower than that in the miR-NC group. (**D**) The tumors in the miR-330-3p-mimics group were markedly smaller than those in the miR-NC group. **Indicated P<0.05.

invasion and migration of GC cells by suppressing EMT, which requires further verification. In addition, rescue experiments showed that, compared with miR-330-3p-mimics, the proliferation, the invasion and migration of MKN-45, MGC-803 increased significantly and EMT remarkably enhanced after simultaneous overexpression of miR-330-3p and PRRX1 or simultaneous underexpression of miR-330-3p and PRRX1, suggesting that there were close ties between miR-330-3p and PRRX1. Therefore, the interrelation between miR-330-3p and PRRX1 was further assessed by dual-luciferase reporter assay, which demonstrated that the overexpression of miR-330-3p notably downregulated the luciferase activity of pmirglo-PRRX1-3 'UT Wt, without effect on that of pmirglo-PRRX1-3′ UTR Mut. Moreover, PRRX1 expression was markedly reduced in miR-330-3p-mimics transfected cells, while remarkably elevated in miR-330-3p-inhibitor-transfected ones, indicating a targeted regulatory connection between miR-330-3p and PRRX1. Through the experiments mentioned above, it is preliminarily proved that up-regulated miR-330-3p expression can inhibit the PRRX1 expression, thus affecting the biological function of GC cells. The specific pathway through which it is regulated, however, remains unclear.

Previous studies believed that Wnt signaling pathway remained to be one of the primary signaling pathways implicated in EMT, as well as one of the essential pathways involved in cell invasion and migration.[20,21] Some others[22] found that PRRX1 could promote invasion, migration and EMT of breast cancer cells by stimulating Wnt/β-catenin signaling pathway in breast cancer cells. The Wnt/β-catenin signaling pathway-related proteins in GC cells treated with over-expressed and under-expressed of miR-330-3p and PRRX1 were detected in the present study. It was found that the PRRX1, p-GSK-3β, β-catenin, cyclinD1, N-cadherin and vimentin expressions were markedly abated, while the expression of GSK-3β, p-β-catenin, E-cadherin were significantly boosted in MKN-45 and MGC-803 cells

transfected with the over-expressed miR-330-3p or under-expressed PRRX1 and vise vista, suggesting that miR-330-3p could inhibit the phosphorylation of GSK-3β protein by regulating PRRX1 and promote the phosphorylation of β-catenin to suppress the activation of Wnt/β-catenin signal pathway, thus inhibiting the EMT of cells. Previous reports[23] also revealed that the activation of Wnt/β-catenin signaling pathway could enhance the proliferation and invasion of GC cells. In addition, studies[24] revealed that miR-519d of different sizes could inhibit the activation of Wnt/β-catenin signaling pathway in GC cells by targeting Twist1 to further inhibit the EMT of GC cells, which all validate the findings in the current study. However, this study also has some shortcomings. For example, due to the small number of cases and the limited time of sample collection, the prognosis of patients cannot be further analyzed. Besides, though there have been many reports on the mechanism of miRNA in gastric cancer, its upstream and downstream mechanism remains elusive, which is another end in our future research. In the future experiments, we will further increase the number of cases, expand the inclusion time of cases and carry out more basic experiments, so as to address the shortcomings of our study.

In conclusion, miR-330-3p can affect the invasion, migration and EMT of GC cells by targeting PRRX1 mediated Wnt/β-catenin signaling pathway, which is expected to be a clinical target for the diagnosis and treatment of GC.

Acknowledgment

This study was financially supported by the Training Program of the Research Fund of the National Foundation of Gansu Provincial Hospital (19GSYPYA-5).

Disclosure

The authors report no conflicts of interest in this work.

References

1. Xiong G, Yang L, Chen Y, Fan Z. Linc-POU3F3 promotes cell proliferation in gastric cancer via increasing T-reg distribution. *Am J Transl Res*. 2015;7(11):2262–2269.
2. Kang M, Ren MP, Zhao L, Li CP, Deng MM. miR-485-5p acts as a negative regulator in gastric cancer progression by targeting flotillin-1. *Am J Transl Res*. 2015;7(11):2212–2222.
3. Liang J, Liu X, Xue H, Qiu B, Wei B, Sun K. MicroRNA-103a inhibits gastric cancer cell proliferation, migration and invasion by targeting c-Myb. *Cell Prolif*. 2015;48(1):78–85. doi:10.1111/cpr.2015.48.issue-1
4. Xia P, Song CL, Liu JF, Wang D, Xu XY. Prognostic value of circulating CD133(+) cells in patients with gastric cancer. *Cell Prolif*. 2015;48(3):311–317. doi:10.1111/cpr.12175
5. Gan HH, Gunsalus KC. The role of tertiary structure in microRNA target recognition. *Methods Mol Biol*. 2019;1970:43–64.
6. Guo LL, Song CH, Wang P, Dai LP, Zhang JY, Wang KJ. Competing endogenous RNA networks and gastric cancer. *World J Gastroenterol*. 2015;21(41):11680–11687. doi:10.3748/wjg.v21.i41.11680
7. Wei CH, Wu G, Cai Q, et al. MicroRNA-330-3p promotes cell invasion and metastasis in non-small cell lung cancer through GRIA3 by activating MAPK/ERK signaling pathway. *J Hematol Oncol*. 2017;10(1):125. doi:10.1186/s13045-017-0493-0
8. Jin Z, Jia B, Tan L, Liu Y. miR-330-3p suppresses liver cancer cell migration by targeting MAP2K1. *Oncol Lett*. 2019;18(1):314–320. doi:10.3892/ol.2019.10280
9. Shimozaki K, Clemenson GD Jr, Gage FH. Paired related homeobox protein 1 is a regulator of stemness in adult neural stem/progenitor cells. *J Neurosci*. 2013;33(9):4066–4075. doi:10.[illegible]/JNEUROSCI.4586-12.2013
10. Guo J, Fu Z, Wei J, Lu W, Feng [illegible] Zhang S. PRRX1 promotes epithelial-mesenchymal transition through the Wnt/beta-catenin pathway in gastric cancer. *Med Oncol*. 20[illegible]32(1):393. doi:10.1007/s12032-014-0393-x
11. Wu J, Li H, Shi M, et al. TET1-mediated DNA hydroxymethylation activates inhibitors of the Wnt/beta-catenin signaling pathway to suppress EMT in pancreatic tumor cells. *J Exp Clin Cancer Res*. 2019;38(1):348. doi:10.1186/s13046-019-1334-5
12. He H, Wu [illegible], Sun Z, Chai L. MiR-4429 prevented gastric cancer progression through targeting METTL3 to inhibit m(6)A-caused stabilization of SEC62. *Biochem Biophys Res Commun*. 2019;517(4):581–587. doi:10.1016/j.bbrc.2019.07.058
13. [illegible] F, Huang J, Liu J, Xu W, Yuan Z. Multivariate analysis of clinicopathological and prognostic significance of miRNA 106b~25 cluster in gastric cancer. *Cancer Cell Int*. 2019;19(1):200. doi:10.1186/s12935-019-0918-7
14. Liu X, [illegible] H, Liu B, Li J, Liu Y, Yu B. miR-330-3p controls cell proliferation by targeting early growth response 2 in non-small-cell lung cancer. *Acta Biochim Biophys Sin (Shanghai)*. 2015;47(6):431–440. doi:10.1093/abbs/gmv032
15. Jamali L, Tofigh R, Tutunchi S, et al. Circulating microRNAs as diagnostic and therapeutic biomarkers in gastric and esophageal cancers. *J Cell Physiol*. 2018;233(11):8538–8550. doi:10.1002/jcp.26850
16. Guan A, Wang H, Li X, et al. MiR-330-3p inhibits gastric cancer progression through targeting MSI1. *Am J Transl Res*. 2016;8(11):4802–4811.
17. Takahashi Y, Sawada G, Kurashige J, et al. Paired related homoeobox 1, a new EMT inducer, is involved in metastasis and poor prognosis in colorectal cancer. *Br J Cancer*. 2013;109(2):307–311. doi:10.1038/bjc.2013.339
18. Hardin H, Guo Z, Shan W, et al. The roles of the epithelial-mesenchymal transition marker PRRX1 and miR-146b-5p in papillary thyroid carcinoma progression. *Am J Pathol*. 2014;184(8):2342–2354. doi:10.1016/j.ajpath.2014.04.011
19. Yang XH, Zhuang MK, Xie WH, et al. 12-Lipoxygenase promotes epithelial-mesenchymal transition via the Wnt/beta-catenin signaling pathway in gastric cancer cells. *Onco Targets Ther*. 2019;12:5551–5561. doi:10.2147/OTT.S201373
20. Cojoc M, Peitzsch C, Kurth I, et al. Aldehyde dehydrogenase is regulated by beta-catenin/TCF and promotes radioresistance in prostate cancer progenitor cells. *Cancer Res*. 2015;75(7):1482–1494. doi:10.1158/0008-5472.CAN-14-1924
21. Zhai Y, Iura A, Yeasmin S, et al. MSX2 is an oncogenic downstream target of activated WNT signaling in ovarian endometrioid adenocarcinoma. *Oncogene*. 2011;30(40):4152–4162. doi:10.1038/onc.2011.123
22. Lv ZD, Kong B, Liu XP, et al. miR-655 suppresses epithelial-to-mesenchymal transition by targeting Prrx1 in triple-negative breast cancer. *J Cell Mol Med*. 2016;20(5):864–873. doi:10.1111/jcmm.12770

23. Wu F, Li J, Guo N, Wang XH, Liao YQ. MiRNA-27a promotes the proliferation and invasion of human gastric cancer MGC803 cells by targeting SFRP1 via Wnt/beta-catenin signaling pathway. *Am J Cancer Res*. 2017;7(3):405–416.

24. Yue H, Tang B, Zhao Y, et al. MIR-519d suppresses the gastric cancer epithelial-mesenchymal transition via Twist1 and inhibits Wnt/beta-catenin signaling pathway. *Am J Transl Res*. 2017;9(8):3654–3664.

RETRACTED